Electronic Spectrum of Cobalt-Free Corrins Calculated by TDDFT Method

Maria Jaworska,* Gabriela Kazibut, and Piotr Lodowski

Department of Theoretical Chemistry, University of Silesia, Szkolna 9, PL-40 006 Katowice, Poland

Received: May 21, 2002; In Final Form: September 25, 2002

The electronic spectra of protonated and unprotonated metal-free corrins were calculated by the TDDFT method in the B3LYP version. Two low energy forms were found from geometry optimization for the protonated corrin, as well as for the unprotonated one. The calculated energies of electronic transitions are in good agreement with the experimental spectrum of synthetic corrin. The largest difference is 0.45 eV and the average difference 0.25 eV. The spectrum of the unprotonated corrin is similar to the spectrum of the protonated corrin with more pronounced $n \rightarrow \pi^*$ transitions due to one more lone electron pair on nitrogen atoms.

1. Introduction

The corrin ring is a macrocyclic ring coordinated to cobalt in 12 -class compounds. In 1965 metal-free corrinoids were isolated by Toohey from the photosynthetic bacterium *Chromatium* D.[1] Similar to the vitamin B_{12} compounds, metal-free corrinoids occur as group of related products, not as single individuals (Scheme 1). Metal-free corrinoids are orange-red-colored compounds. Their absorption spectra have the typical α, β, and γ pattern characteristic for the cobalt-containing corrinoids.[2−5] Two relatively weak bands occur in the visible region at 524 and 497 nm and an intense band is present in the upper UV region at 329 nm. The former coincide with the maxima of aquocobamides,[5] the latter is at lower wavelength than in B_{12} vitamins. The similarity of the spectra is considered as an evidence that the main absorption bands in cobalt corrinoids originate from π-transitions in the corrin ring. The bands in the spectra of synthetic corrins are shifted to lower wavelengths (496, 470, and 314 nm for 1,2,2,7,7,12,12-heptamethylcorrin (Scheme 2).[6] Theoretical calculations of spectral properties for model corrins and cobalamins were performed by the use of semiempirical and SCF methods.[8−12,14−17] The electronic spectrum of dicyanocobinamide and cyanocobalamin was calculated by the TDDFT method.[7] The results of the latter calculations show that the model based on π-transitions is not sufficient for describing the full electronic spectrum of dicyanocobinamide and cyanocobalamin.

In this work we calculated electronic spectra of the protonated and unprotonated corrin with the TDDFT method.[18,19] The TDDFT method has been lately widely used for computation of electronic spectra and it was shown that it is reliable for organic and inorganic systems.[20−32]

2. Methods and Computational Details

Calculations were carried out with the use of the DFT and the TDDFT methods with the B3LYP density functional.[33,34] Gaussian98 program[35] was used throughout the calculations. The valence double-ζ basis of Dunning and Huzinaga (D95V)[36] was employed for carbon, nitrogen, and hydrogen. Additional polarization *d* function on carbon with the exponent 0.8 and on nitrogen with the exponent 0.75 were added. These basis sets are of the form (10s5p1d)/[3s2p1d] for carbon and nitrogen and (4s)/[2s] for hydrogen. Full optimization of the structures of cobalt-free corrins was done by the B3LYP method. The calculations of electronic spectrum were performed at the TDDFT level. The molecular structure and orbitals were depicted by program MOLDEN.[37]

SCHEME 1

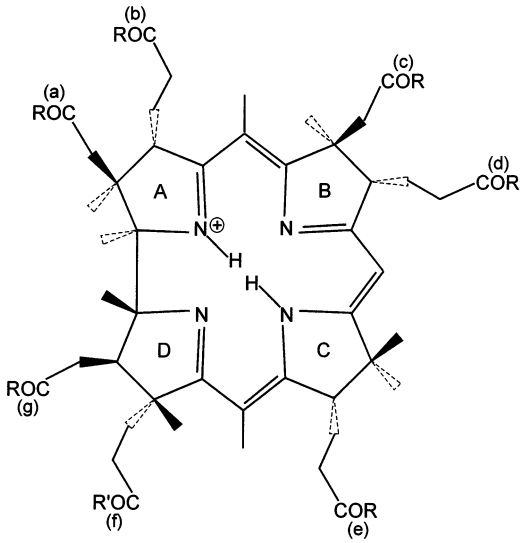

1 Hydrogenobyrinic acid R = R' = OH

2 Hydrogenobyric acid R = NH_2, R' = OH

3 Hydrogenobinamide R = NH_2, R' = $-NH-CH_2-CH(CH_3)-OH$

4 Hydrogenobamide R = NH_2, R' = $-NH$, R'' = OH

SCHEME 2

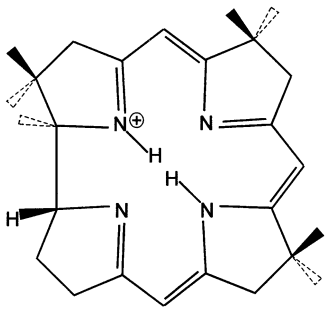

10.1021/jp021261t CCC: $25.00
Published on Web 02/11/2003

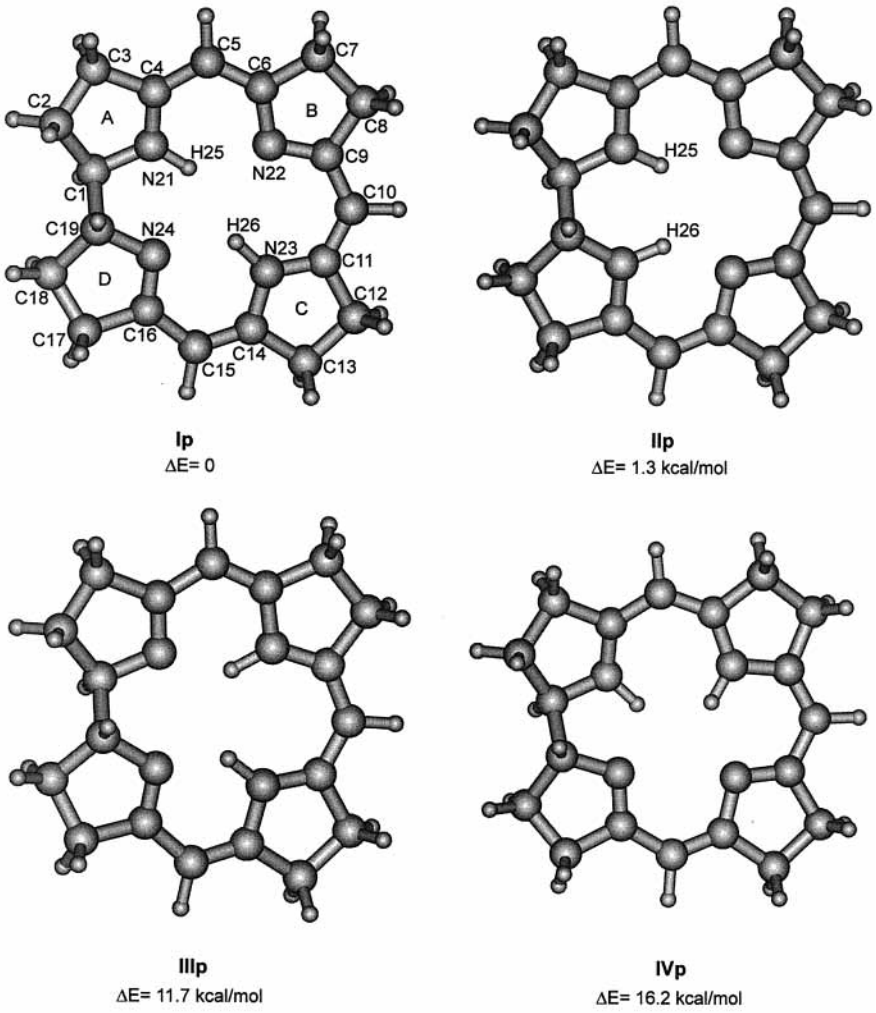

Figure 1. The optimized structures of four forms of the protonated corrin.

TABLE 1: Calculated Values of the Geometrical Parameters for the Protonated Cobalt-Free Corrins[a]

	r [Å]										
bond	**Ip**	**IIp**	exptl	bond angles	**Ip**	**IIp**	exptl		torsion angles	**Ip**	**IIp**	exptl
C1−N21	1.46	1.46	1.49	C2−C1−C19	93.4	116.0	113		C1−N21−C4−C5	176.2	179.0	172
C4−N21	1.32	1.33	1.29	C1−C19−C18	116.7	116.0	117		N21−C4−C5−C6	−4.6	−2.9	−25
C6−N22	1.37	1.36	1.38	C17−C18−C19	102.9	104.9	105		C4−C5−C6−N22	−1.0	−0.1	−3
C9−N22	1.34	1.35	1.32	C1−C2−C3	104.8	104.9	102		C5−C6−N22−C9	179.3	−179.7	178
C11−N23	1.35	1.35	1.38	C1−N21−C4	116.7	116.1	115		C6−N22−C9−C10	178.7	178.5	179
C14−N23	1.39	1.36	1.35	N21−C4−C5	123.0	122.7	125		N22−C9−C10−C11	−4.0	−4.6	−4
C16−N24	1.30	1.33	1.29	C4−C5−C6	123.5	122.1	125		C9−C10−C11−N23	−3.0	−4.5	−3
C19−N24	1.47	1.46	1.47	C5−C6−N22	124.5	122.8	123		C10−C11−N23−C14	179.3	178.6	179
C1−C2	1.55	1.55	1.57	C6−N22−C9	109.3	109.9	108		C11−N23−C14−C15	179.2	−179.8	177
C2−C3	1.56	1.56	1.55	N22−C9−C10	125.7	126.3	124		N23−C14−C15−C16	0.1	−0.1	2
C3−C4	1.51	1.51	1.50	C9−C10−C11	127.9	128.9	125		C14−C15−C16−N24	0.3	−2.7	−2
C4−C5	1.42	1.41	1.42	C10−C11−N23	127.1	126.2	126		C15−C16−N24−C19	−177.6	179.1	177
C5−C6	1.39	1.40	1.35	C11−N23−C14	115.1	109.9	115		C16−N24−C19−C1	−141.3	−135.5	−120
C6−C7	1.52	1.52	1.54	N23−C14−C15	123.5	122.8	124		N24−C19−C1−N21	−37.3	−40.9	−45
C7−C8	1.54	1.54	1.52	C14−C15−C16	123.5	122.1	124		C19−C1−N21−C4	−134.8	−135.3	−94
C8−C9	1.52	1.52	1.49	C15−C16−N24	122.2	122.7	121	↑	C1−C2−C3−C4	−21.2	−20.7	26
C9−C10	1.41	1.40	1.40	C16−N24−C19	110.3	116.1	110		C2−C3−C4−N21	15.9	14.4	−13
C10−C11	1.39	1.40	1.34	N24−C19−C1	108.3	109.6	108	A	C3−C4−N21−C1	−3.9	−1.7	−7
C11−C12	1.52	1.52	1.53	C19−C1−N21	108.0	109.6	105		C4−N21−C1−C2	−10.0	−11.7	23
C12−C13	1.55	1.54	1.54					↓	N21−C1−C2−C3	18.9	19.5	−28
C13−C14	1.52	1.52	1.51					↑	C6−C7−C8−C9	−4.5	−3.5	−8
C14−C15	1.36	1.40	1.35						C7−C8−C9−N22	4.2	3.7	7
C15−C16	1.46	1.41	1.46					B	C8−C9−N22−C6	−1.9	−2.2	−2
C16−C17	1.52	1.51	1.50						C9−N22−C6−C7	−1.4	−0.3	−3
C17−C18	1.55	1.55	1.54					↓	N22−C6−C7−C8	3.9	2.6	7
C18−C19	1.55	1.55	1.54					↑	C11−C12−C13−C14	−4.5	−3.6	−18
C1−C19	1.55	1.55	1.55						C12−C13−C14−N23	3.7	2.7	15
N21−H25	1.02	1.03						C	C13−C14−N23−C11	−1.4	−0.4	−5
N23−H26	1.03								C14−N23−C11−C12	−1.7	−2.2	−7
N24−H26		1.03						↓	N23−C11−C12−C13	3.9	3.7	16
								↑	C16−C17−C18−C19	−20.9	−20.9	7
									C17−C18−C19−N24	22.6	19.7	−8
								D	C18−C19−N24−C16	−15.5	−11.9	6
									C19−N24−C16−C17	1.2	−1.7	−2
								↑	N24−C16−C17−C18	13.4	14.4	−3

[a] The experimental values for 1,2,2,7,7,12,12-heptamethylcyanocorrin are shown (ref 38).

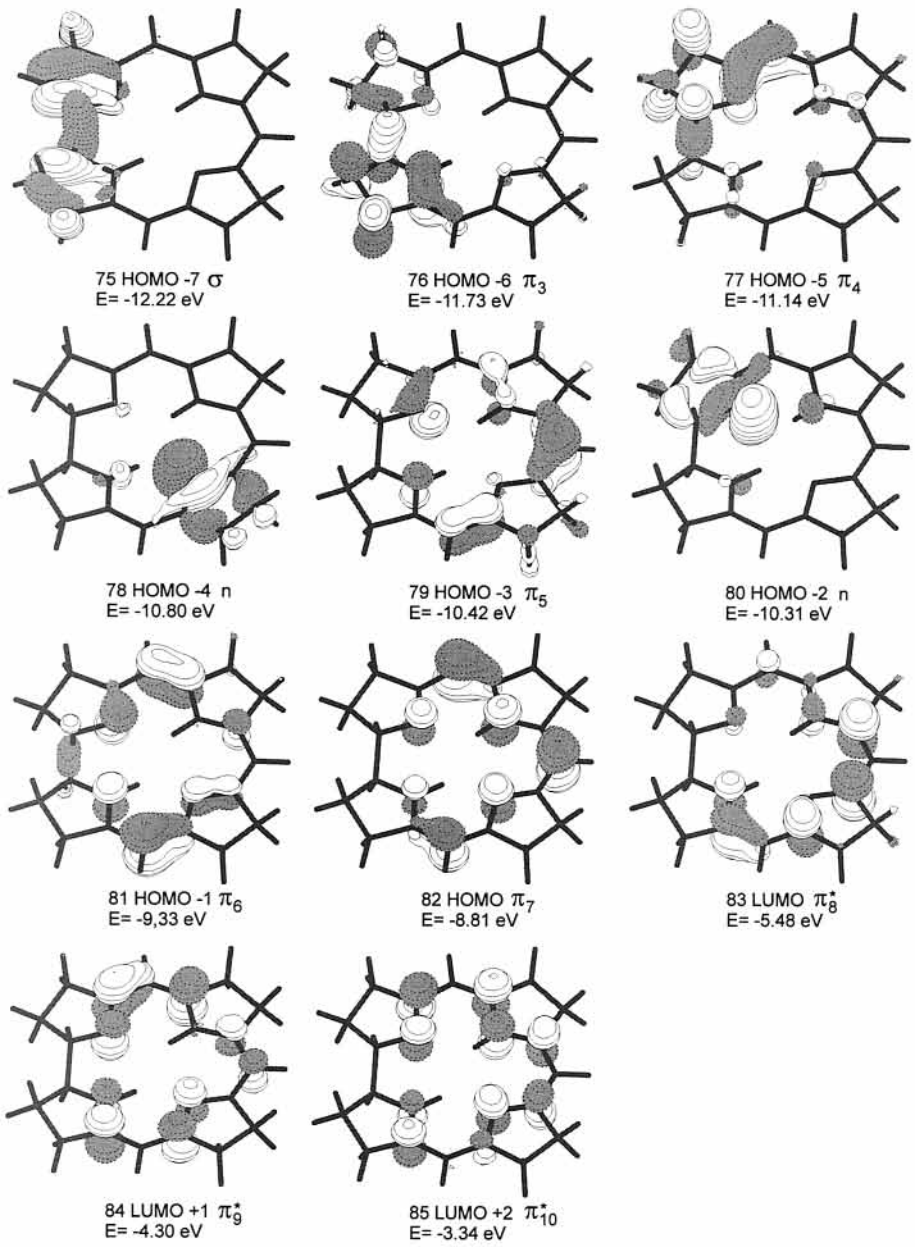

Figure 2. The molecular orbitals active in the electronic transitions of the protonated corrin, form **Ip**.

3. Results and Discussion

Metal-free natural and synthetic corrins occur in the protonated form in the solid state and in the acidic solution. After neutralization with alkali at first the unprotonated form is obtained, next the conjugated π-bonded system of the corrin ring is interrupted and a lactam product is formed.[2]

The calculations were performed for the protonated and unprotonated corrin ring. We used a model system without any side chains at the corrin ring. The spin allowed, singlet transitions were calculated. The spectra obtained from TDDFT method were compared with the experimental spectra of hydrogenobalamin[2] and synthetic 1,2,2,7,7,12,12-heptamethylcorrin.[6]

3.1. Protonated Corrin. *3.1.1. Molecular Geometry.* The calculations were performed with the use of crystallographic data as a starting geometry. Structures with all possible distributions of two protons among four nitrogen atoms were optimized. There are four such structures (**Ip**−**IVp**), and they are presented in Figure 1. In the crystal structure the two protons are bound to the nitrogen atoms at rings A and C.[38] The structure **Ip** in Figure 1 has the lowest energy, and it corresponds to the crystallographic structure. The form **IIp** is higher in energy only of 1.3 kcal. In solution both forms may exist in equilibrium. The energy of two other forms (**IIIp** and **IVp**) is considerably higher than that of **Ip** (11.7 and 16.2 kcal, respectively). The geometry parameters for **Ip** and **IIp** are gathered in Table 1. The experimental geometry is shown for comparison.[38]

The calculated bond lengths are in good agreement with the experiment. The largest differences between the calculated and the experimental values occur for the C14−N23, C5−C6, and C10−C11 bonds (0.04−0.05 Å). The largest difference in bond angles amounts to 19.6° for the angle C2−C1−C19. The most pronounced differences between the optimized and the experimental structural parameters occur for torsional angles, where N21−C4−C5−C6, C16−N24−C19−C1, and C19−C1−N21−C4 differ from the experiment of 20.4°, 21.3°, and 40.8°, respectively. The optimized structure of **Ip** is more planar then the crystallographic structure around A and D rings. The

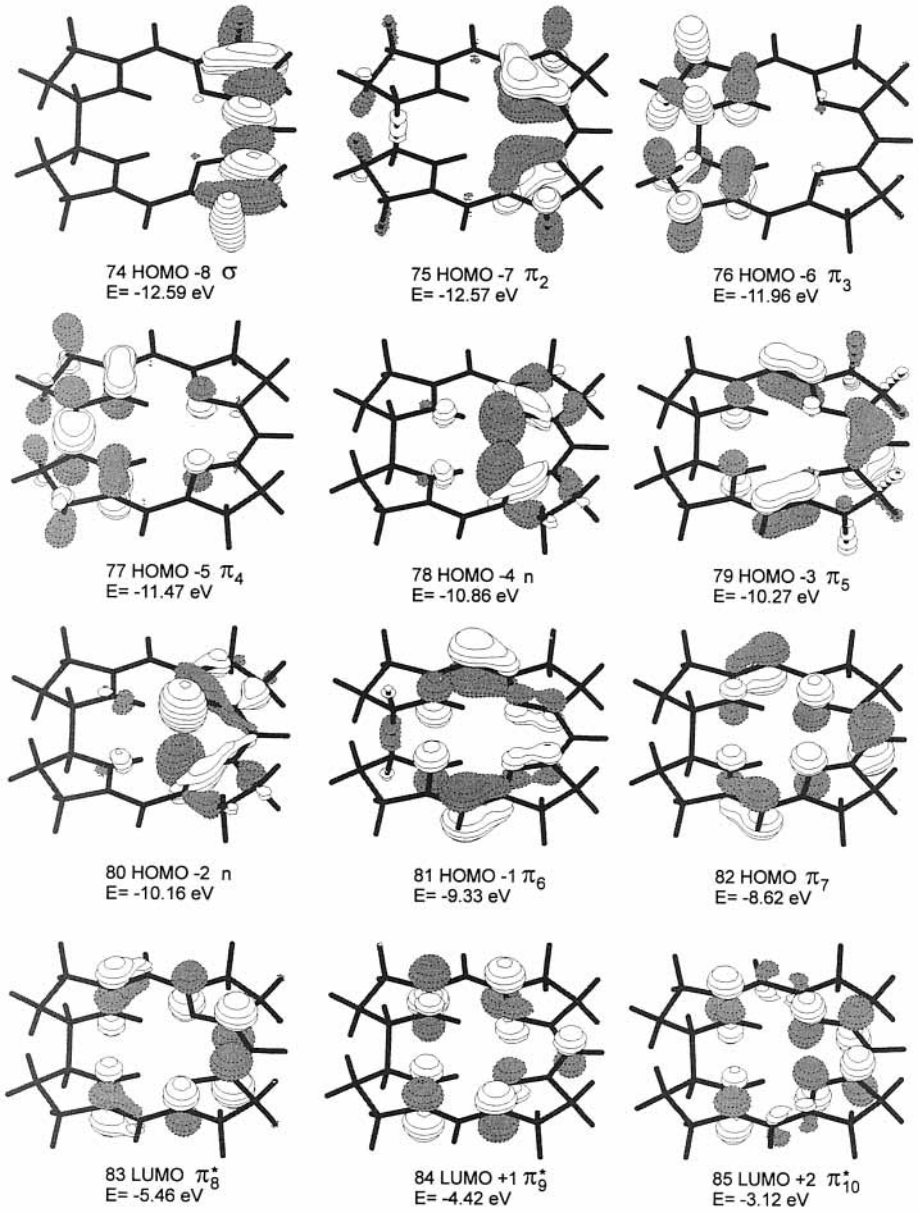

Figure 3. The molecular orbitals active in the electronic transitions of the protonated corrin, form **IIp**.

calculated conformation of A and D rings is not so strongly folded as the experimental one.

The geometry parameters of **IIp** are close to that of **Ip**, except for the angle C2−C1−C19 which for **IIp** is closer to experimental value than that for **Ip** (Table 1).

3.1.2. Electronic Spectrum. There are 13 carbon atoms with 14 electrons in the conjugated π-electron system of corrin. According to the theoretical interpretation based on PPP calculations,[11,12] bands in the visible and near UV part of the spectra of corrinoids result from excitations between the two highest occupied π orbitals (π_6 and π_7) and the two lowest unoccupied ones (π_8^* and π_9^*). We calculated the spin allowed, singlet transitions for **Ip** and **IIp**. Since **Ip** and **IIp** are close in energy, the both forms should contribute to the electronic spectrum. The energies of **IIIp** and **IVp** are much higher (11.7 and 16.2 kcal, Figure 1), and we assumed that their contribution to the electronic spectrum is negligible. The molecular orbitals active in electronic transitions are presented in Figures 2 and 3 for the forms **Ip** and **IIp**, respectively. The calculated singlet transition energies (and the respective wavelengths) together with the oscillator strengths for **Ip** and **IIp** are gathered in Table 2. The experimental wavelengths for hydrogenobalamin and 1,2,2,7,7,12,12-heptamethylcorrin are shown also in Table 2. For comparison the experimental wavelengths were recalculated to excitation energies in eV. In what follows, we compare the calculated transition energies to the experimental ones of 1,2,2,7,7,12,12-heptamethylcorrin. The comparison to a synthetic corrin is more appropriate since the side chains in natural corrins may influence the spectrum to larger extend than methyl groups. The calculated spectrum is presented also in Figure 4. The transitions of both forms **Ip** and **IIp** were placed on the plot of the calculated spectrum, where the heights of the bars denoting transitions are proportional to oscillator strengths. Additionally each transition was approximated by a Gauss curve with the height equal to oscillator strength and some arbitrary width equal to 0.06.

Usually, the dicyanocobinamide spectrum is used as reference standard for corrinoid compounds,[13] the most intense bands in the natural and synthetic corrins are shifted toward higher energies comparing to it. In the experimental spectrum two bands are present at 495 and 472 nm for 1,2,2,7,7,12,12-heptamethylcorrin. They coincide with the α,β band of dicy-

TABLE 2: Calculated Wavelengths, Excitation Energies, and Oscillator Strengths for the Protonated Cobalt-Free Corrin (Numbers 74−82 Denote HOMO Orbitals, 83−85 Denote LUMO Orbitals)

excited state			λ [nm] (ΔE [eV])	f	exptl λ [nm] (ΔE [eV]) synthetic corrin[a]	hydrogenobalamin[b]	
1	**IIp**	0.64 **82**(π_7) → **83**(π_8^*)	452.9 (2.74)	0.2398	495(2.51)	524(2.37)	α, β
2	**Ip**	0.64 **82**(π_7) → **83**(π_8^*)	428.3 (2.89)	0.1992	472(2.63)	497(2.49)	
3	**Ip**	0.62 **81**(π_6) → **83**(π_8^*) +0.29 **82**(π_7) → **84**(π_9^*)	362.6 (3.42)	0.0914	384(3.23), 360(3.45),	415(2.99), 392(3.16),	D, E, γ
4	**IIp**	0.58 **81**(π_6) → **83**(π_8^*) −0.39 **82**(π_7) → **84**(π_9^*)	362.5 (3.42)	0.0397	346(3.59)	377(3.29)	
5	**IIp**	0.69 **80**(n) → **83**(π_8^*)	340.8 (3.64)	0.0000			
6	**Ip**	0.63 **80**(n) → **83**(π_8^*) −0.21 **78**(n) → **83**(π_8^*)	307.7 (4.03)	0.0014			
7	**IIp**	0.52 **82**(π_7) → **84**(π_9^*) +0.29 **81**(π_6) → **83**(π_8^*)	298.7 (4.15)	0.6822	311(3.99)	329(3.77)	δ
8	**Ip**	0.66 **78**(n) → **83**(π_8^*) +0.23 **80**(n) → **83**(π_8^*)	297.5 (4.17)	0.0012			
9	**IIp**	0.52 **81**(π_6) → **84**(π_9^*) +0.46 **79**(π_5) → **83**(π_8^*)	294.3 (4.21)	0.0009			
10	**Ip**	0.48 **82**(π_7) → **84**(π_9^*) +0.25 **81**(π_6) → **84**(π_9^*) −0.36 **79**(π_5) → **83**(π_8^*)	291.2 (4.26)	0.2434	300(4.14)	318(3.90)	
11	**IIp**	0.64 **78**(n) → **83**(π_8^*) +0.26 **80**(n) → **84**(π_9^*)	289.5 (4.28)	0.0319			
12	**Ip**	0.44 **81**(π_6) → **84**(π_9^*) −0.33 **82**(π_7) → **84**(π_9^*) −0.30 **79**(π_5) → **83**(π_8^*)	283.3 (4.38)	0.3002			
13	**IIp**	0.43 **79**(π_5) → **83**(π_8^*) +0.37 **82**(π_7) → **85**(π_{10}^*) −0.38 **81**(π_6) → **84**(π_9^*)	275.7 (4.50)	0.1240			
14	**Ip**	0.42 **82**(π_7) → **85**(π_{10}^*) −0.38 **81**(π_6) → **84**(π_9^*) −0.36 **79**(π_5) → **83**(π_8^*)	269.6 (4.60)	0.1731	286(4.34)	290(4.28)	
15	**IIp**	0.64 **80**(n) → **84**(π_9^*) −0.26 **78**(n) → **83**(π_8^*)	256.1 (4.84)	0.0006			
16	**Ip**	0.64 **80**(n) → **84**(π_9^*)	249.4 (4.97)	0.0016			
17	**Ip**	0.62 **77**(π_4) → **83**(π_8^*) +0.22 **82**(π_7) → **85**(π_{10}^*)	243.3 (5.09)	0.0908			
18	**Ip**	0.45 **82**(π_7) → **85**(π_{10}^*) +0.21 **79**(π_5) → **83**(π_8^*) +0.20 **81**(π_6) → **84**(π_9^*) -0.28 **77**(π_4) → **83**(π_8^*)	236.7 (5.24)	0.4025	259(4.79)	272(4.56)	
19	**IIp**	0.56 **82**(π_7) → **85**(π_{10}^*)	236.6 (5.24)	0.4161			
20	**IIp**	0.59 **79**(π_5) → **84**(π_9^*) −0.35 **77**(π_4) → **83**(π_8^*)	233.7 (5.31)	0.1179			
21	**Ip**	0.61 **81**(π_6) → **85**(π_{10}^*) +0.25 **79**(π_5) → **84**(π_9^*)	228.8 (5.42)	0.0624		240(5.17)	
22	**IIp**	0.65 **78**(n) → **84**(π_9^*) +0.21 **80**(n) → **85**(π_{10}^*)	227.8 (5.44)	0.0080			
23	**IIp**	0.52 **77**(π_4) → **83**(π_8^*) +0.36 **81**(π_6) → **85**(π_{10}^*) +0.29 **79**(π_5) → **84**(π_9^*)	226.9 (5.46)	0.0363			
24	**Ip**	0.65 **78**(n) → **84**(π_9^*)	224.9 (5.51)	0.0045			
25	**Ip**	0.45 **79**(π_5) → **84**(π_9^*) +0.40 **76**(π_3) → **83**(π_8^*)	220.4 (5.63)	0.0914			
26	**IIp**	0.56 **81**(π_6) → **85**(π_{10}^*) −0.28 **77**(π_4) → **83**(π_8^*)	217.9 (5.69)	0.0047			
27	**Ip**	0.55 **76**(π_3) → **83**(π_8^*) −0.33 **79**(π_5) → **84**(π_9^*)	216.4 (5.73)	0.0082			
28	**IIp**	0.69 **76**(π_3) → **83**(π_8^*)	209.3 (5.92)	0.0052			
29	**Ip**	0.64 **80**(n) → **85**(π_{10}^*)	205.0 (6.05)	0.0016			
30	**IIp**	0.62 **80**(n) → **85**(π_{10}^*) −0.23 **78**(n) → **84**(π_9^*)	204.7 (6.06)	0.0032			
31	**Ip**	0.67 **75**(σ) → **83**(π_8^*)	204.0 (6.08)	0.0001			
32	**IIp**	0.67 **74**(σ) → **83**(π_8^*)	200.9 (6.17)	0.0032			

[a] 1,2,2,7,7,12,12-Heptamethylcorrin from ref 6. [b] Hydrogenobalamin from ref 2.

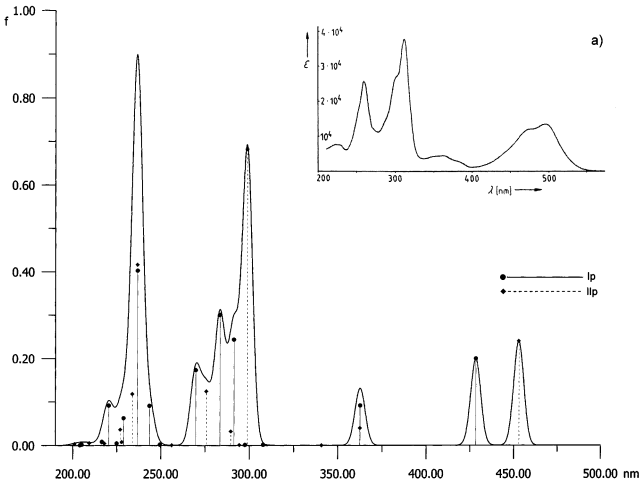

Figure 4. The calculated electronic spectrum of **Ip** and **IIp**. (a) The experimental spectrum from ref 6.

anocobinamide, and are of medium intensity. These two bands can be compared to the calculated transitions at 452.9 nm (form **IIp**) and 428.3 nm (form **Ip**). Both transitions come from the $\pi_7 \rightarrow \pi_8^*$ excitation. The energy difference between the calculated transitions and 1,2,2,7,7,12,12-heptamethylcorrin bands is 0.23 and 0.26 eV.

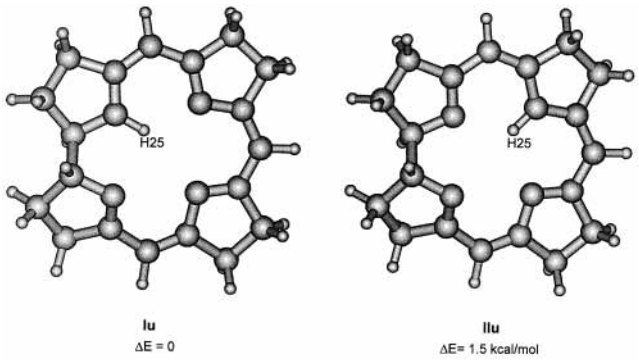

Figure 5. Optimized structures of two forms of the unprotonated corrin.

The next bands in the experimental spectrum are at 384, 360, and 346 nm for 1,2,2,7,7,12,12-heptamethylcorrin. These bands have small intensity and are in the same range as D, E, and γ bands in dicyanocobinamide. In the calculated spectrum the transitions at 362.6 nm with the oscillator strength 0.0914 (**Ip**) and 362.5 nm with the oscillator strength 0.0397 (**IIp**) may be ascribed to these bands. They are symmetric and antisymmetric combinations of the $\pi_6 \rightarrow \pi_8^*$ and $\pi_7 \rightarrow \pi_9^*$ transitions for **Ip**

TABLE 3: Calculated Values of the Geometrical Parameters for the Unprotonated Cobalt-Free Corrins

	r [Å]								
bond	**Iu**	**IIu**	bond angles	**Iu**	**IIu**		torsion angles	**Iu**	**IIu**
C1−N21	1.46	1.46	C2−C1−C19	116.6	90.8		C1−N21−C4−C5	−174.6	−179.4
C4−N21	1.33	1.29	C1−C19−C18	113.4	112.8		N21−C4−C5−C6	4.7	0.6
C6−N22	1.33	1.38	C17−C18−C19	103.2	102.7		C4−C5−C6−N22	−0.7	0.6
C9−N22	1.36	1.37	C1−C2−C3	104.1	103.8		C5−C6−N22−C9	177.5	175.3
C11−N23	1.32	1.31	C1−N21−C4	115.0	111.0		C6−N22−C9−C10	−176.6	179.2
C14−N23	1.38	1.39	N21−C4−C5	125.7	121.6		N22−C9−C10−C11	0.1	0.6
C16−N24	1.29	1.29	C4−C5−C6	122.0	123.1		C9−C10−C11−N23	−1.6	−0.2
C19−N24	1.46	1.46	C5−C6−N22	122.1	125.4		C10−C11−N23−C14	178.6	178.5
C1−C2	1.55	1.56	C6−N22−C9	110.5	114.4		C11−N23−C14−C15	176.6	176.6
C2−C3	1.55	1.55	N22−C9−C10	124.7	126.6		N23−C14−C15−C16	−3.7	−3.3
C3−C4	1.52	1.52	C9−C10−C11	126.6	125.1		C14−C15−C16−N24	−28.0	−31.8
C4−C5	1.40	1.46	C10−C11−N23	125.6	123.6		C15−C16−N24−C19	171.5	172.2
C5−C6	1.41	1.36	C11−N23−C14	109.7	109.7		C16−N24−C19−C1	−106.7	−103.0
C6−C7	1.53	1.52	N23−C14−C15	124.4	125.1		N24−C19−C1−N21	−36.8	−33.4
C7−C8	1.55	1.55	C14−C15−C16	124.4	125.2		C19−C1−N21−C4	−143.5	−135.6
C8−C9	1.53	1.52	C15−C16−N24	123.4	123.4	↑	C1−C2−C3−C4	−23.2	−15.2
C9−C10	1.38	1.37	C16−N24−C19	110.3	109.7		C2−C3−C4−N21	42.1	10.7
C10−C11	1.44	1.44	N24−C19−C1	107.6	109.2	A	C3−C4−N21−C1	3.4	−0.6
C11−C12	1.53	1.53	C19−C1−N21	111.6	111.3		C4−N21−C1−C2	−18.3	−9.9
C12−C13	1.54	1.54				↓	N21−C1−C2−C3	24.6	15.7
C13−C14	1.53	1.53				↑	C6−C7−C8−C9	2.3	−13.2
C14−C15	1.37	1.36					C7−C8−C9−N22	−3.2	10.3
C15−C16	1.46	1.46				B	C8−C9−N22−C6	2.7	−2.9
C16−C17	1.53	1.53					C9−N22−C6−C7	−1.1	−6.1
C17−C18	1.55	1.55				↓	N22−C6−C7−C8	−1.0	12.1
C18−C19	1.56	1.56				↑	C11−C12−C13−C14	−10.2	−10.3
C1−C19	1.55	1.56					C12−C13−C14−N23	10.3	10.4
N21−H25	1.03					C	C13−C14−N23−C11	−5.5	−5.6
N22−H25		1.03					C14−N23−C11−C12	−2.0	−2.0
						↓	N23−C11−C12−C13	8.3	8.3
						↑	C16−C17−C18−C19	13.8	19.1
							C17−C18−C19−N24	−17.8	−23.4
						D	C18−C19−N24−C16	15.4	18.8
							C19−N24−C16−C17	−6.1	−5.9
						↑	N24−C16−C17−C18	−5.7	−9.4

and **IIp**, respectively. The calculated transition energy compares well with the central band of the *D, E,* and γ bands (the energy difference relative to 1,2,2,7,7,12,12-heptamethylcorrinis 0.04 eV).

The band with the highest intensity in corrins occurs at 311 nm in 1,2,2,7,7,12,12-heptamethylcorrin. It coincides with the δ band of dicyanocobinamide. In the calculated spectrum the transition at 298.7 nm of **IIp** may be ascribed to this band. It has the oscillator strength equal to 0.6822. It is a symmetric combination of the $\pi_7 \rightarrow \pi_9^*$ and $\pi_6 \rightarrow \pi_8^*$ excitations, with a larger participation of the first one. The energy difference between the calculated transition and the transition of 1,2,2,7,7,-12,12-heptamethylcorrin is 0.16 eV.

The calculated transitions at 291.2 nm (the oscillator strength 0.2434) and 283.3 nm (the oscillator strength 0.3002) for **Ip** may be compared to the band at 300 nm for 1,2,2,7,7,12,12-heptamethylcorrin. They are symmetric and antisymmetric combinations of the $\pi_6 \rightarrow \pi_9^*$ and $\pi_7 \rightarrow \pi_9^*$ transitions plus an admixture of the $\pi_5 \rightarrow \pi_8^*$ transition. The energy difference between the experimental transition and the calculated one is 0.24 eV.

The transition at 269.6 nm in the calculated spectrum (form **Ip**) may be related to the experimental band at 286 nm in 1,2,2,7,7,12,12-heptamethylcorrin. The calculated transitions is a mixture of the $\pi_7 \rightarrow \pi_{10}^*$, $\pi_6 \rightarrow \pi_9^*$ and $\pi_5 \rightarrow \pi_8^*$ excitations. The energy difference between the calculated and experimental transitions is 0.26 eV.

The calculations show a transition for **Ip** at 236.7 nm with the oscillator strength 0.4025 and for **IIp** at 236.6 with the oscillator strength 0.4161. This transitions can be compared to the experimental band with the high intensity band at 259 nm in 1,2,2,7,7,12,12-heptamethylcorrin. The energy difference between the calculated and the experimental transition is 0.45 eV. This transition results mainly from the $\pi_7 \rightarrow \pi_{10}^*$ excitation in the both forms plus some other high $\pi \rightarrow \pi^*$ excitations for **Ip**.

There are several $n \rightarrow \pi^*$ transitions in the calculated spectrum of the protonated corrin. The lowest energy one occurs at 340.8 nm (in form **IIp**). All these transition have very small or zero oscillator strengths. The $n \rightarrow \pi^*$ transition with the largest oscillator strength (0.0319) occurs at 289.5 nm (form **IIp**).

The calculated spectrum of protonated corrin (form **Ip** and **IIp**) is in good agreement with the experimental one. The bands up to the band are described by excitations among four orbitals π_6, π_7, π_8^* and π_9^* . This is in accord with the interpretation of the spectra of corrinoids based on semiempirical calculations. The bands at lower wavelengths are mainly higher $\pi \rightarrow \pi^*$ excitations. $n \rightarrow \pi^*$ excitations occur in the calculated spectrum of protonated corrin with small oscillator strengths. The position of calculated transitions agree well with the experimental data for the synthetic corrin, 1,2,2,7,7,12,12-heptamethylcorrin, the largest difference being 0.45 eV for the highest energy transition and the average difference about 0.25 eV.

3.2. Neutral Corrin. *3.2.1. Geometry.* There are two possible forms of the unprotonated corrin which differ in the position of the proton attached to a nitrogen atom. They are shown in Figure 5. The full optimization of both structures was performed. The optimized geometry parameters are shown in Table 3. There is no experimental structural data for unprotonated corrins, as far as we know. The comparison of optimized geometry parameters of **Iu** and **IIu** with those for **Ip** and **IIp** (Table 1) shows that the conformation of the corrin ring in the unprotonated corrins is different from the conformation in the protonated corrins, which is indicated by large differences in torsional angles.

3.2.2. Electronic Spectrum. After adding alkali to the solution of corrins, changes in the electronic spectrum occur depending on pH of the solution.[2] They are related to deprotonation of the corrin ring, and conversion to the a lactam product.

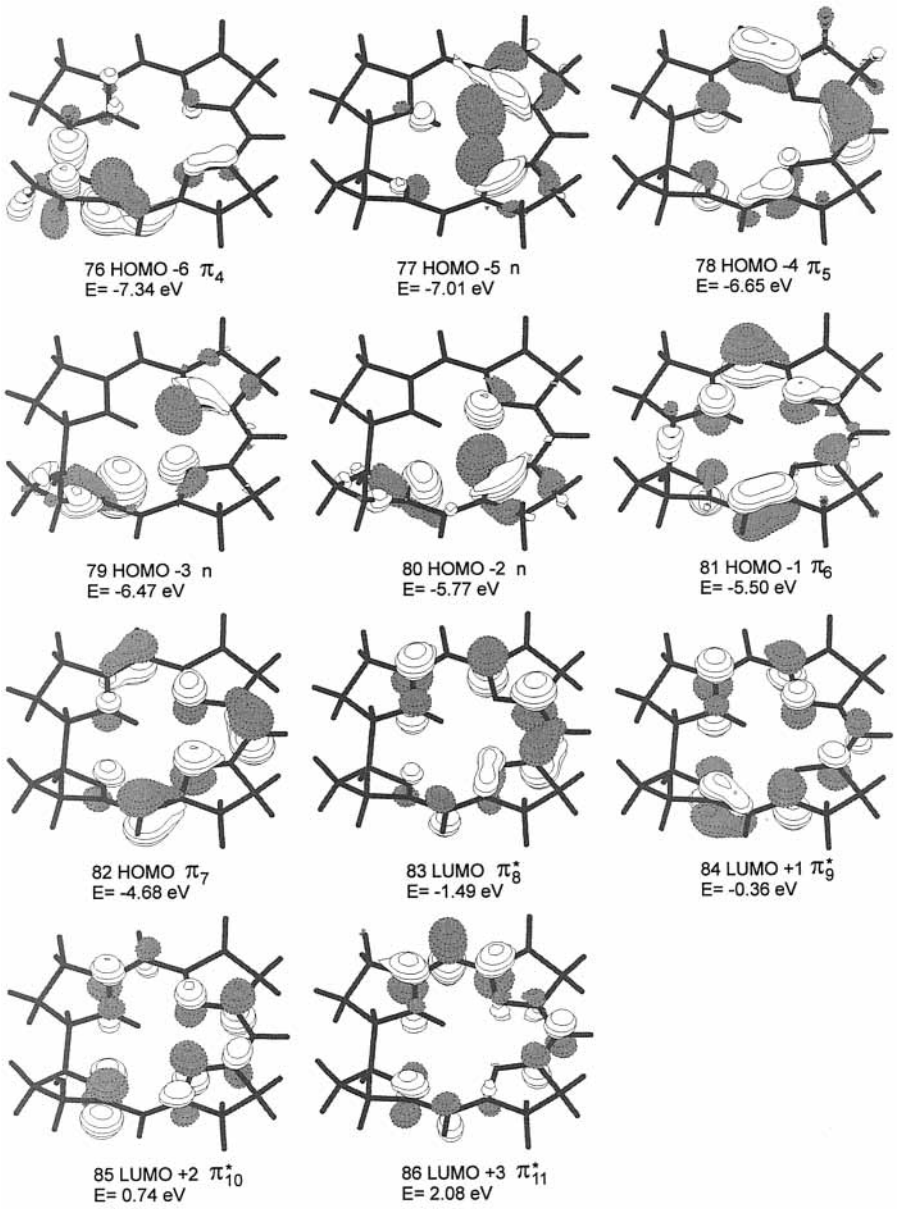

Figure 6. The molecular orbitals active in the electronic transitions of the unprotonated corrin, form **Iu**.

We calculated electronic transitions for both unprotonated forms **Iu** and **IIu** (Figure 5) The energy difference between **Iu** and **IIu** is small (1.5 kcal), and we assumed, similarly as in the case of the protonated corrin, that the spectrum can come from transitions occurring in both of them. The molecular orbitals active in electronic transitions are shown in Figures 6 and 7 for **Iu** and **IIu**, respectively. The calculated electronic transitions are collected in Table 4. The calculated electronic spectrum is presented in Figure 8. The calculated spectrum for the neutral forms of corrin is very similar to that for the protonated forms, the main differences are related with shifting the transitions toward slightly shorter wavelengths and somewhat smaller oscillator strengths. The transitions at 446.5 nm (**Iu**) and 410.2 nm (**IIu**) are the $\pi_7 \rightarrow \pi_8^*$ transitions. They have medium oscillator strengths of 0.1894 and 0.1525, respectively. The transitions at 373.5 nm (**Iu**) and 345.6 nm (**IIu**) are mainly $n \rightarrow \pi^*$ transitions. The transitions at 357.1 nm (**Iu**) and 339.9 nm (**IIu**) are antisymmetric and symmetric combination of $\pi_7 \rightarrow \pi_9^*$ and $\pi_6 \rightarrow \pi_8^*$ excitations. All these transitions have rather small oscillator strengths. The transitions with high oscillator strengths at 293.5 nm (**Iu**) and 286.9 nm (**IIu**) are symmetric and antisymmetric combinations of the $\pi_6 \rightarrow \pi_8^*$ and $\pi_7 \rightarrow \pi_9^*$ respectively, with a substantial admixture of a $n \rightarrow \pi^*$ excitation. The transitions at 272.2 nm (**Iu**) and 260.5 nm (**IIu**) originate from $n \rightarrow \pi^*$ excitation and higher $\pi \rightarrow \pi^*$ excitations, respectively. The transitions at 238.5 nm (the oscillator strength 0.3093) and 234.8 nm (the oscillator strength 0.1939) for **Iu** come from higher $\pi \rightarrow \pi^*$ excitations. The transitions at 237.9 nm (oscillator strength 0.1036) and 233.4 nm (oscillator strength 0.2913) for **IIu** come from higher $\pi \rightarrow \pi^*$ excitations plus an $n \rightarrow \pi^*$ excitation. The transitions at 213.8 nm (**Iu**, $f = 0.0886$) and 208.6 nm (**IIu**, $f = 0.1098$) are high $\pi \rightarrow \pi^*$ excitations.

Generally the calculated spectrum for the unprotonated corrin is very similar to that of the protonated corrin. There is larger participation of $n \rightarrow \pi^*$ excitations in the electronic transitions with respectively larger oscillator strengths. This can be understood, as in the protonated corrin two lone pairs of the four nitrogen atoms are engaged in bonding with hydrogen atoms, while in the unprotonated corrin only one. There are three *n* orbitals among the HOMO orbitals of **Iu** and **IIu** and only two for **Ip** and **IIp**.

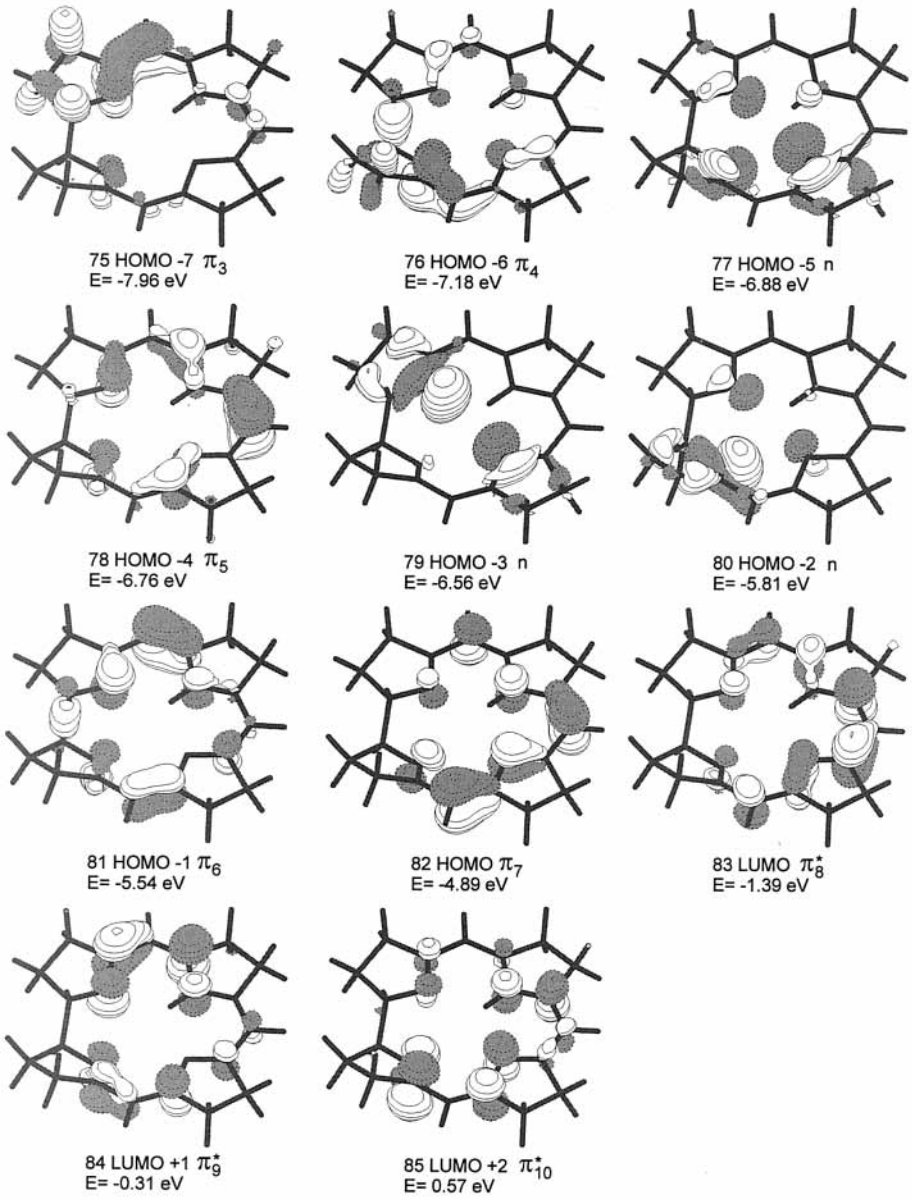

Figure 7. The molecular orbitals active in electronic the transitions of the unprotonated corrin, form **IIu**.

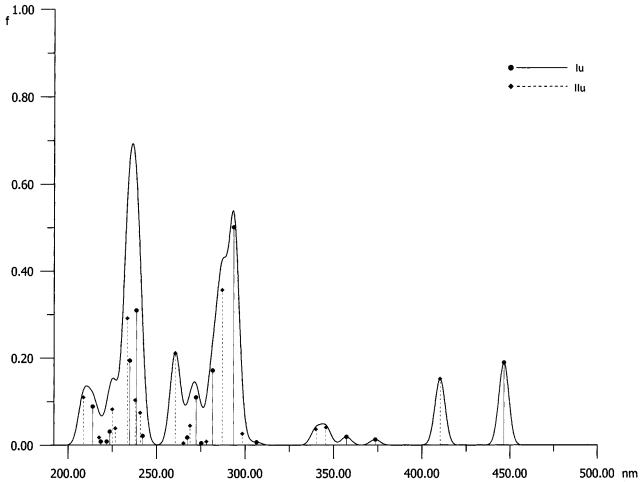

Figure 8. The calculated electronic spectrum of **Iu** and **IIu**.

4. Conclusions

We calculated the electronic spectrum of the protonated and unprotonated corrin with TDDFT method in B3LYP version. For both protonated and unprotonated corrins there are two forms close in energy ($\Delta E = 1.3$ for the former one and 1.5 kcal for the latter). The low energy forms may exist in equilibrium in solution and contribute to the electronic spectrum. In addition, at neutral pH equilibrium may exist between the protonated and unprotonated forms. The spectra of the protonated and unprotonated forms are similar to each other. The main calculated transitions between 450 and 290 nm originate from the excitations between π_6, π_7 and π_8^*, π_9^* orbitals, although other electronic transitions are also involved. Thus the low energy part of electronic spectrum obtained from TDDFT calculations for the metal-free corrins generally agrees with four-orbital model emerging from semiempirical calculations for corrinoid compounds.[11,12] The transitions at higher energies are mainly higher $\pi \rightarrow \pi^*$ excitations. In the unprotonated corrin the $n \rightarrow \pi^*$ transitions play significant role, due to the presence of one more nitrogen lone electron pair in this system.

Acknowledgment. The Gaussian 98 calculations were carried out in Wrocław Supercomputing Center, WCSS, Wrocław, Poland, under calculational Grant No. 51/96.

TABLE 4: Calculated Wavelengths, Excitation Energies, and Oscillator Strengths for the Unprotonated Cobalt-free Corrin (Numbers 75−82 Denote HOMO Orbitals, 83−86 Denote LUMO Orbitals)

excited state			λ [nm] (ΔE [eV])	f
1	**Iu**	0.63 **82**(π_7) → **83**(π_8^*)	446.5 (2.78)	0.1894
2	**IIu**	0.64 **82**(π_7) → **83**(π_8^*)	410.2 (3.02)	0.1525
3	**Iu**	0.67 **80**(n) → **83**(π_8^*)	373.5 (3.32)	0.0131
4	**Iu**	0.55 **81**(π_6) → **83**(π_8^*) −0.43 **82**(π_7) → **84**(π_9^*)	357.1 (3.47)	0.0192
5	**IIu**	0.64 **80**(n) → **83**(π_8^*) −0.21 **81**(π_6) → **83**(π_8^*)	345.6 (3.59)	0.0414
6	**IIu**	0.55 **81**(π_6) → **83**(π_8^*) +0.37 **82**(π_7) → **84**(π_9^*)	339.9 (3.65)	0.0368
7	**Iu**	0.64 **79**(n) → **83**(π_8^*)	306.4 (4.05)	0.0070
8	**IIu**	0.61 **79**(n) → **83**(π_8^*)	298.4 (4.15)	0.0266
9	**Iu**	0.43 **82**(π_7) → **84**(π_9^*) +0.30 **80**(n) → **84**(π_9^*) + 0.30 **81**(π_6) → **83**(π_8^*)	293.5 (4.22)	0.5014
10	**IIu**	0.48 **82**(π_7) → **84**(π_9^*) −0.25 **81**(π_6) → **83**(π_8^*) −0.23 **79**(n) → **83**(π_8^*)	286.9 (4.32)	0.3566
11	**Iu**	0.49 **77**(n) → **83**(π_8^*) −0.28 **80**(n) → **84**(π_9^*)	281.6 (4.40)	0.1717
12	**IIu**	0.52 **77**(n) → **83**(π_8^*) −0.37 **80**(n) → **84**(π_9^*)	278.1 (4.46)	0.0086
13	**Iu**	0.53 **81**(π_6) → **84**(π_9^*) +0.41 **78**(π_5) → **83**(π_8^*)	275.2 (4.50)	0.0049
14	**Iu**	0.50 **80**(n) → **84**(π_9^*) −0.34 **77**(n) → **83**(π_8^*)	272.2 (4.55)	0.1098
15	**IIu**	0.47 **81**(π_6) → **84**(π_9^*) −0.46 **78**(π_5) → **83**(π_8^*)	268.9 (4.61)	0.0448
16	**Iu**	0.49 **82**(π_7) → **85**(π_{10}^*) +0.39 **78**(π_5) → **83**(π_8^*) −0.23 **81**(π_6) → **84**(π_9^*)	267.3 (4.64)	0.0177
17	**IIu**	0.39 **80**(n) → **84**(π_9^*) +0.29 **77**(n) → **83**(π_8^*) −0.35 **82**(π_7) → **85**(π_{10}^*)	265.2 (4.67)	0.0048
18	**IIu**	0.39 **82**(π_7) → **85**(π_{10}^*) +0.33 **80**(n) → **84**(π_9^*) −0.29 **81**(π_6) → **84**(π_9^*)	260.5 (4.76)	0.2114
19	**Iu**	-0.61 **79**(n) → **84**(π_9^*)	242.0 (5.12)	0.0215
20	**IIu**	0.44 **79**(n) → **84**(π_9^*) +0.23 **76**(π_4) → **83**(π_8^*) −0.32 **80**(n) → **85**(π_{10}^*) −0.21 **78**(π_5) → **83**(π_8^*)	240.6 (5.15)	0.0743
21	**Iu**	0.37 **76**(π_4) → **83**(π_8^*) +0.31 **82**(π_7) → **85**(π_{10}^*) −0.28 **78**(π_5) → **83**(π_8^*)	238.5 (5.20)	0.3093
22	**IIu**	0.61 **76**(π_4) → **83**(π_8^*)	237.9 (5.21)	0.1036
23	**Iu**	0.55 **76**(π_4) → **83**(π_8^*) −0.27 **82**(π_7) → **85**(π_{10}^*)	234.8 (5.28)	0.1939
24	**IIu**	0.41 **79**(n) → **84**(π_9^*) +0.30 **78**(π_5) → **83**(π_8^*) +0.29 **82**(π_7) → **85**(π_{10}^*)	233.4 (5.31)	0.2913
25	**IIu**	0.46 **81**(π_6) → **85**(π_{10}^*) −0.35 **80**(n) → **85**(π_{10}^*) −0.22 **79**(n) → **84**(π_9^*)	226.6 (5.47)	0.0389
26	**IIu**	0.46 **81**(π_6) → **85**(π_{10}^*) +0.34 **80**(n) → **85**(π_{10}^*)	224.9 (5.51)	0.0823
27	**Iu**	0.52 **80**(n) → **85**(π_{10}^*) −0.34 **77**(n) → **84**(π_9^*)	223.4 (5.55)	0.0312
28	**Iu**	0.55 **81**(π_6) → **85**(π_{10}^*) +0.39 **78**(π_5) → **84**(π_9^*)	221.7 (5.59)	0.0085
29	**Iu**	0.54 **77**(n) → **84**(π_9^*) +0.36 **80**(n) → **85**(π_{10}^*)	218.4 (5.68)	0.0082
30	**IIu**	0.60 **77**(n) → **84**(π_9^*) −0.25 **80**(n) → **85**(π_{10}^*)	217.5 (5.70)	0.0177
31	**Iu**	0.51 **78**(π_5) → **84**(π_9^*) +0.23 **82**(π_7) → **86**(π_{11}^*) −0.29 **81**(π_6) → **85**(π_{10}^*)	213.8 (5.80)	0.0886
32	**IIu**	0.51 **78**(π_5) → **84**(π_9^*) +0.39 **75**(π_3) → **83**(π_8^*)	208.6 (5.94)	0.1098

References and Notes

(1) Toohey, J. I. *Proc. Nat. Sci.* **1965**, *54*, 934.

(2) Koppenhagen, V. B. Metal-Free Corrinoids and Metal Insertion. In *B_{12}*; Dolphin, D., Ed.; John Wiley and Sons: New York, 1982; Vol. 1, pp 105−149.

(3) Koppenhagen, V. B.; Pfiffner, J. J. *J. Biol. Chem.* **1971**, *246*, 3075.

(4) Schlingmann, G.; Koppenhagen, V. B. *Proceedings of the Third European Symposium on Vitamin B_{12} and Intrinsic Factor*, Zürich, Switzerland, 1979; de Gruyer: Berlin, 1979; pp 149−154.

(5) Gianotti, C. Electronic Spectra of B_{12} and Related Systems. In *B_12*; Dolphin, D., Ed.; John Wiley and Sons: New York, 1982; Vol. 1, pp 393−430.

(6) Lewis, N. J.; Pfaltz, A.; Eschenmoser, A. *Angew. Chem.* **1983**, *95*, 743−744 7. Andruniow, T.; Kozlowski, P. M.; Zgierski, M. Z. *J. Chem. Phys.* **2001**, *115*, 7522−7533.

(7) Andruniow, T.; Kozlowski, P. M.; Zgierski, M. Z. *J. Chem. Phys.* **2001**, *115*, 7522−7533.

(8) Kuhn, H.; Drexhage, K. H.; Martin, H. *Proc. R. Soc.* **1965**, 288, 350.

(9) Offenhartz, B. *Proc. R. Soc. A* **1965**, *288*, 350.

(10) Veillard, A.; Pullman, B. *J. Theor. Biol.* **1965**, *8*, 307.

(11) Day, P. *Theor. Chim. Acta* **1967**, *7*, 328−341.

(12) Day, P. *Coord. Chem. Rev.* **1967**, *2*, 109.

(13) Reference 5, p 413.

(14) Offenhartz, P. O.; Offenhartz, B. H.; Fung, M. M. *J. Am. Chem. Soc.* **1970**, *92*, 2966.

(15) Schrauzer, G. N. *Näturwissenschaften* **1969**, *53*, 459.

(16) Schrauzer, G. N.; Lee, L. P.; Sibert, J. W. *J. Am. Chem. Soc.* **1970**, *92*, 2966.

(17) Salem, L.; Eisenstein, O.; Anh, T. A.; Burgi, H. B.; Devaquet, A.; Segal, G.; Veillard, A. *Nouv. J. Chim.* **1977**, *1*, 335−348.

(18) Casida, M. E. Time-Dependent Density Functional Response Theory for Molecules. In *Recent Advances in Density Functional Methods*; Chong, D. P., Ed.; World Scientific: Singapore, 1995; Vol. 1, pp 155−192.

(19) Casida, M. E. Time-Dependent Density Functional Response Theory for Molecular Systems: Theory, Computational Methods, and Functionals. In *Recent Developments and Applications of Modern Density Functional Theory, Theoretical and Computational Chemistry*; Seminario, J. M., Ed.; Elsevier B. V.: Amsterdam, 1996; pp 391−439.

(20) Jamorski, C.; Casida, M. E.; Salahub, D. R. *J. Chem. Phys.* **1996**, *104*, 5134−5147.

(21) Stratmann, R. E.; Scuseria, G. E.; Frisch, M. J. *J. Chem. Phys.* **1998**, *109*, 8218−8224.

(22) Hirata, S.; Lee, T. J.; Head-Gordon, M. *J. Chem. Phys.* **1999**, *111*, 8904−8912.

(23) van Gisbergen, S. J. A.; Rosa, A.; Riccardi, G.; Baerends, E. J. *J. Chem. Phys.* **1999**, *111*, 2499−2506.

(24) Fabian, J. *Theor. Chem. Acc.* **2001**, *106*, 199−217.

(25) Boulet, P.; Chermette, H.; Daul, C.; Gilardoni, F.; Rogemont, F.; Weber, J.; Zuber, G. *J. Phys. Chem. A* **2001**, *105*, 885−894.

(26) Rosa, A.; Riccardi, G.; Baerends, E. J.; van Gisbergen, S. J. A. *J. Phys. Chem. A* **2001**, *105*, 3311−3327.

(27) van Gisbergen, S. J. A.; Groeneveld, J. A.; Rosa, A.; Snijders, J. G.; Baerends, E. J. *J. Phys. Chem. A* **1999**, *103*, 6835−6844.

(28) Gorelsky, S. I.; Lever, A. B. P. *Int. J. Quantum Chem.* **2000**, *80*, 636−645.

(29) Full, J.; González, L.; Daniel, C. *J. Phys. Chem. A* **2001**, *105*, 184−189.

(30) Adamo, C.; Barone, V. *Theor. Chem. Acc.* **2000**, *105*, 169−172.

(31) Nguyen, K. A.; Pachter, R. *J. Chem. Phys.* **2001**, *114*, 10757−10767.

(32) Brocławik, E.; Borowski, T. *Chem. Phys. Lett* **2001**, *339*, 433−437.

(33) Becke, A. D. *J. Chem. Phys.* **1993**, *98*, 5648−5652.

(34) Stevens, P. J.; Devlin, F. J.; Chablowski, C. F.; Frisch, M. J. *J. Phys. Chem.* **1994**, *98*, 11623−11627.

(35) Frisch, M. J.; Trucks, G. W.; Schlegel, H. B.; Scuseria, G. E.; Robb, M. A.; Cheeseman, J. R.; Zakrzewski, V. G.; Montgomery, J. A. Jr.; Stratmann, R. E.; Burant, J. C.; Dapprich, S.; Millam, J. M.; Daniels, A. D.; Kudin, K. N.; Strain, M. C.; Farkas, O.; Tomasi, J.; Barone, V.; Cossi, M.; Cammi, R.; Mennucci, B.; Pomelli, C.; Adamo, C.; Clifford, S.; Ochterski, J.; Petersson, G. A.; Ayala, P. Y.; Cui, Q.; Morokuma, K.; Malick, D. K.; Rabuck, A. D.; Raghavachari, K.; Foresman, J. B.; Cioslowski, J.; Ortiz, J. V.; Stefanov, B. B.; Liu, G.; Liashenko, A.; Piskorz, P.; Komaromi, I.; Gomperts, R.; Martin, R. L.; Fox, D. J.; Keith, T.; Al-Laham, M. A.; Peng, C. Y.; Nanayakkara, A.; Gonzalez, C.; Challacombe, M.; Gill, P. M. W.; Johnson, B.; Chen, W.; Wong, M. W.; Andres, J. L.; Gonzalez, C.; Head-Gordon, M.; Replogle, E. S.; Pople, J. A. *Gaussian 98*, revision A.11; Gaussian, Inc.: Pittsburgh, PA, 1998.

(36) Dunning, T. H., Jr.; Hay, P. J. In *Methods of Electronic Structure Theory*; Schaeffer, H. F., III, Ed.; Plenum Press: New York, 1977; pp 1−27.

(37) Schaftenaar, G. *Molden, Release 3.6*; CMBI, Netherlands (2000), www.caos.kun.nl/∼schft/molden/molden.html.

(38) Glusker, J. P. X-ray Crystallography of B_{12} and Cobaloximes. In *B_{12}*; Dolphin, D., Ed.; John Wiley and Sons: New York, 1982; Vol. 1, pp 23−105.